MASSACHUSETTS INSTITUTE OF TECHNOLOGY

LINCOLN LABORATORY

PREDICTION OF OPTICAL LANDING GUIDANCE SYSTEM PERFORMANCE IN CAT. III-a MINIMUM WEATHER

D. G. KOCHER

Group 42

TECHNICAL NOTE 1973-47

8 NOVEMBER 1973

LEXINGTON MASSACHUSETTS

The work reported in this document was performed at Lincoln Laboratory, a center for research operated by Massachusetts Institute of Technology, with the support of the Department of the Air Force under Contract F19628-73-C-0002.

Abstract

The feasibility of using a laser optical system to provide precision guidance for the final two miles of aircraft landing approaches in low visibility weather is examined. Since low visibility is caused most frequently by clouds and fog, approximate calculations of the optical signal, scattered light and noise are made as a function of range for various cloud and fog densities. It is concluded that with current laser technology, performance of an optical landing guidance system would be inadequate in the presence of Category III-a minimum visibility clouds and fogs.

Accepted for the Air Force
Eugene C. Raabe, Lt. Col., USAF
Chief, ESD Lincoln Laboratory Project Office

Preface

The increasing size and speed of aircraft, together with the desire for all weather operation, has created a need for landing guidance systems of increased accuracy during periods of low visibility. The work reported here was performed to see if the general area of laser technology offered any solutions to the problem of providing high accuracy landing guidance signals in low visibility weather.

TABLE OF CONTENTS

Prediction of Optical Landing Guidance System Performance in Cat. III-a Minimum Weather

I. INTRODUCTION

To land airplanes during Cat III-a weather minimums (700 foot runway visible range), the landing guidance system (LGS) must be capable of supplying the airplane with extremely accurate position information. Because of the complexity of an RF system which can provide sufficiently precise guidance, a system operating at optical wavelengths sometimes is suggested as an alternative. Unfortunately, optical systems suffer from appreciable propagation scattering and absorption during those periods of low visibility when the LGS is needed most.

In this note the performance of a hypothetical optical LGS is estimated for various weather conditions down to 0.1 nautical mile (n. m.) visual (2% contrast) visibility, which corresponds to 900 foot runway visible range in daytime with Step 5 approach lighting. This is done by determining the signal, noise and scattered light power as a function of range and visibility using representative LGS propagation medium models. Operating wavelengths from the visible to the far infrared are considered, although calculations are performed only for 10.6 μm, the wavelength believed most suitable for this application.

II. THE OPTICAL LGS MODEL

An optical LGS might be designed several different ways. As a reference point, computations are performed first for a "baseline" system which is a straight forward optical analog of a scanning microwave LGS. The performance of various other optical LGS techniques then are considered in a later section by treating them as perturbations of the baseline system.

It is assumed the baseline optical LGS is being used to measure airplane elevation. A fan-shaped scanning beam is assumed (See Fig. 1). The beam is transmitted from a location near the runway to a receiver in the airplane. Elevation position is derived from timing of the maximum signal intensity as the beam

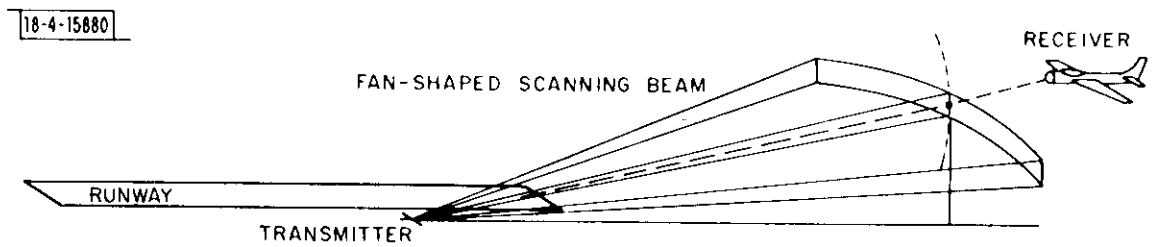

Fig. 1. Fan-shaped scanning beam assumed for the optical LGS model.

sweeps past the receiver, or alternatively, from modulation on the beam. (A second orthogonal beam is used similarly to supply azimuth position to the airplane.) A simple fixed field-of-view (FOV) receiver in the airplane is assumed.

The operational range considered is approximately two miles since the system would be used only for the final portions of the landing approach. To this range must be added the distance at which the transmitter is placed behind the runway threshold. The range referred to in the remainder of this note is the range from the transmitter to the receiver.

An accuracy of 1.4 feet (2σ) at a range of 3000 feet and an angular coverage of $\pm$ 20 degrees azimuth and 0 to +20 degrees elevation are typical for improved landing guidance systems, and these values are assumed in the optical LGS model. The scanning beamwidth is chosen so that the 2σ position accuracy at 3,000 feet range is maintained. This requires a beamwidth of 0.5×10^{-3} radians. Twenty updates per second are assumed. Assuming the airplane receiver is used to detect the peak of the beam intensity as it sweeps by, it can be shown that a bandwidth of 2×10^{4} Hz is required if equal time is provided for interleaving azimuth fan beam sweeps.

III. THE PROPAGATION MEDIUM

The propagation medium (atmosphere) can influence the performance of the optical LGS through extinction of the fan beam by absorption and by scattering. Both absorption and scattering result from the particulates, e.g., aerosols, fog, cloud, rain and snow. In addition, molecular absorption by the gaseous atmospheric components also occurs. The relative importance of these various phenomena changes with wavelength and visibility. In this note, the runway visible range is the parameter used to describe the condition of the atmosphere, since airport operations are governed by runway visual range.

For runway visual ranges less than 3827 feet, Allard's Law is used to compute the attenuation coefficient γ (See Appendix A). For example, when the runway visual range is 700 feet, the visible light attenuation coefficient is 54.5/n.m. (attenuation 128 dB/km) during daytime operations and twice as large (109/n.m. or 256 dB/km) during night operations. Since the laser beam transmission T equals $e^{-\gamma R}$, it is clear

that an optical LGS operating at visible wavelengths must tolerate a great attenuation of the signal and also must tolerate it in the presence of significant background light in the receiver FOV, such as that from sunlit fog or clouds.

The amount of absorption and scattering depends on the wavelength and the condition causing the reduced visibility. At the risk of oversimplifying the problem, the principal trends are summarized in Fig. 2 for water droplet sizes ranging from hazes to rain and snow. Fog, cloud, rain and snow are the scattering particles most often responsible for Cat III-a minimums. Since rain and snow particles generally are larger than 0.5 mm, the attenuation coefficient γ for rain and snow is approximately constant over the wavelength region considered in Fig. 2. In addition, simple considerations show that in the case of rain the attenuation is relatively small even for moderate rainfall rates. For example, at 2.5 cm/hour rainfall rate, typical values of drop diameter and drop terminal velocity are 2 mm and 7m/sec, respectively. A straightforward calculation gives the optical attenuation coefficient for rain, since the attenuation coefficient is twice the geometrical cross section per unit volume in this case where the wavelength is much less than the droplet size. This calculation gives an attenuation of 6.5 dB/km for the rain parameters given above, which corresponds to a 2% contrast visibility of 2.6 km. This result is corroborated by reports from practical airport experience that serious reductions in visibility are due to fog much more frequently than to rain. Similar calculations for snow are not so straightforward, but it is to be expected the scattering by snow will be at least as great as for rain since the geometrical cross section of a given amount of water in the form of snow exceeds the cross section in the form of rain. Like rain, snow crystals generally have dimensions large compared to the wavelengths being considered here. Chu and Hogg[1] report that for a given liquid content, attenuation by snow is intermediate between the attenuations due to rain and fog.

In summary, it appears that for this problem attenuation by scattering from rain (and possibly also snow) is not as serious as the attenuation due to fogs and that in the case of rain or snow, no other wavelength in the range being considered offers a substantial advantage over visible light.

On the other hand, for the more frequent and operationally more important case of visibility limited by fogs and clouds there is a significant wavelength dependency. Because serious reductions in visibility are caused most frequently by fog, the remainder

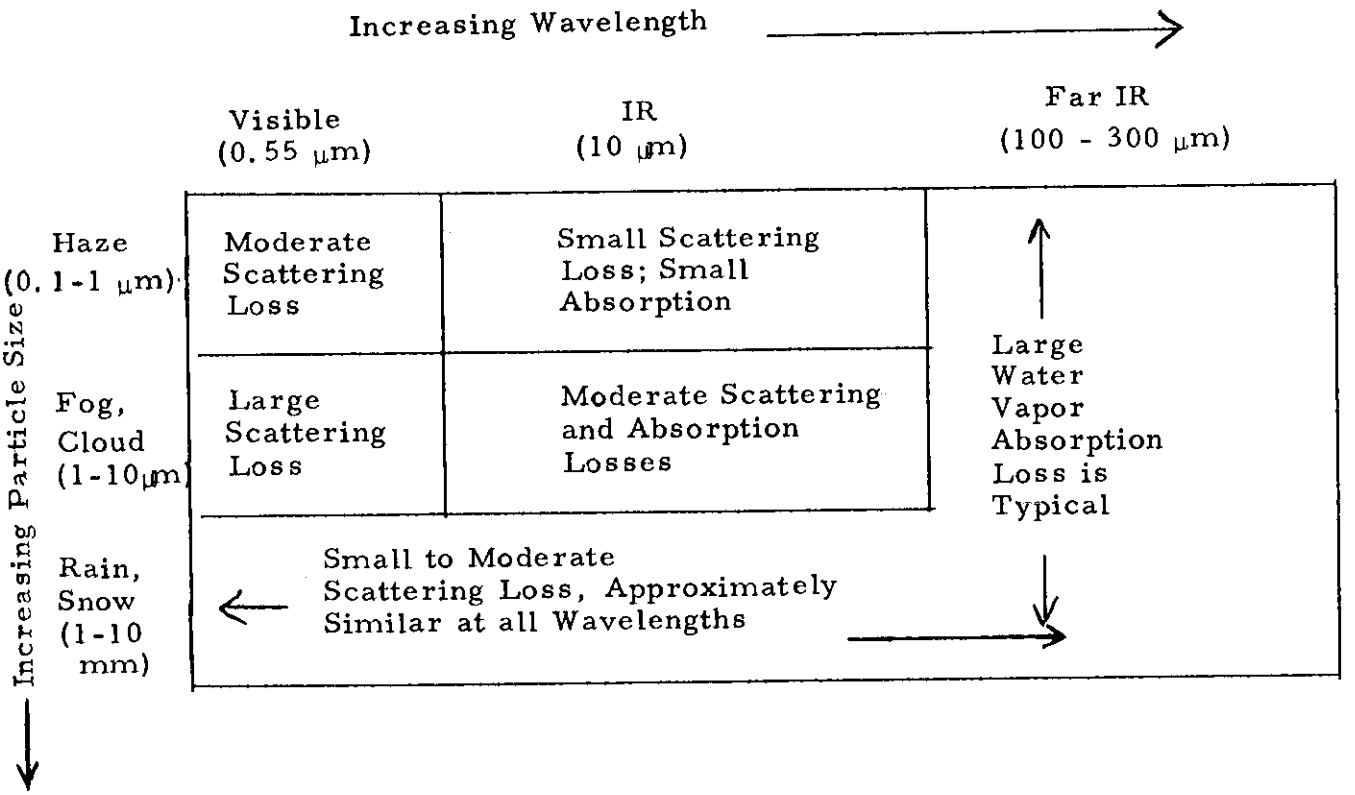

Fig. 2 Predominant extinction phenomena encountered for different kinds of weather.

of this note is restricted to consideration of attenuation by fogs and clouds.

The droplet size distributions of typical fogs and clouds peak in the range 1 μm to 10 μm radius. Since particle scattering efficiency decreases rapidly for wavelengths greater than the particle size, the attenuation by scattering from fog and cloud droplets is significantly less at 10 μm wavelength than at visible wavelengths. However, for wavelengths beyond about 20 μm, absorption by water vapor increases significantly. The availability of significant CO_2 laser power at 10.6 μm makes that wavelength a logical choice for the baseline system. In the next sections, the signal, scattered light and background noise power are calculated for the optical LGS model operating at 10.6 μm in clouds and fogs having attenuation coefficients commensurate with Cat III-a minimum RVR's.

IV. EXTINCTION AND SCATTERING BY FOGS AND CLOUDS

To compute the performance of the optical LGS in fog and cloud, it is necessary to determine (a) the attenuation of the scanning beam (or "signal") and (b) the amount of energy which is scattered out of the beam but still enters the receiver as a source of interference. It is possible to predict these quantities for both visible wavelengths and 10 μm wavelength using data and techniques from the literature. It is assumed here that the fog or cloud is homogeneous, which often is not the case and which could be the source of considerable error.

The characterization of attenuation and scattering by fogs and clouds begins by considering the extinction by individual water droplets. Extinction by single particles is described by the single particle absorption and scattering cross sections, the sum of which is the extinction cross section.

$$\sigma_{abs} + \sigma_{sc} = \sigma_{ext.} \tag{1}$$

Integrating the cross sections over the particle size distributions yields the absorption, scattering and attenuation coefficients α, β and γ, respectively:

$$\alpha + \beta = \gamma \tag{2}$$

The albedo A of the optical medium is the ratio

$$A = \beta/\gamma \tag{3}$$

The quantities in equation (2) are functions of wavelength. It is necessary to determine γ, A and hence α and β for the atmosphere and for representative fogs and clouds at different wavelengths in order to estimate LGS performance.

Hazes, fogs and clouds, in that order, have droplets size distributions peaking at progressively longer wavelengths. Hazes are not considered here since hazes become "evolving fogs" when the water particle density increases to the point where visibility is reduced significantly. A sampling of representative fog and cloud droplet size distributions obtained from measurements is reproduced in Fig. 3. Fog and cloud droplet size distributions vary considerably with atmospheric conditions and the distributions in Fig. 3 should be regarded as approximate. Nevertheless, the following trends are clear. At visible wavelengths, droplet diameters are larger than the wavelength and the scattering cross section is approximately the same as the geometrical cross section of the droplets. At $\lambda = 10\ \mu m$, a considerable proportion of the droplets is less than a wavelength in diameter and the scattering cross section is beginning to decrease significantly. At longer wavelengths, the scattering cross section is even smaller.

In Fig. 4 the computed absorption and scattering cross section[11] of water droplets (per unit volume of water) are plotted for $\lambda = 10.6\ \mu m$. Numerical integration of these cross sections over the drop size distributions for the "Arnulf" fog and "Curcio" cloud in Fig. 3 shows in both cases the integrated absorption and scattering cross sections to be nearly equal. This implies the albedo A of these fogs and clouds is 0.50 at 10.6 μm. Deirmendjian[3] obtained A = 0.60 at 10 μm for the cloud droplet distribution shown in Fig. 3. The value of the albedo is important for computing the scattered light in the receiver FOV.

The absorption by fogs and clouds at visible wavelengths is small. Heggestad[6] has found the albedo of cloud droplets to be 0.96 at visible wavelengths. In the region 100 to 300 μm wavelength it is shown later that for the range of visibilities being considered here, scattering and absorption by cloud and fog droplets is relatively small and

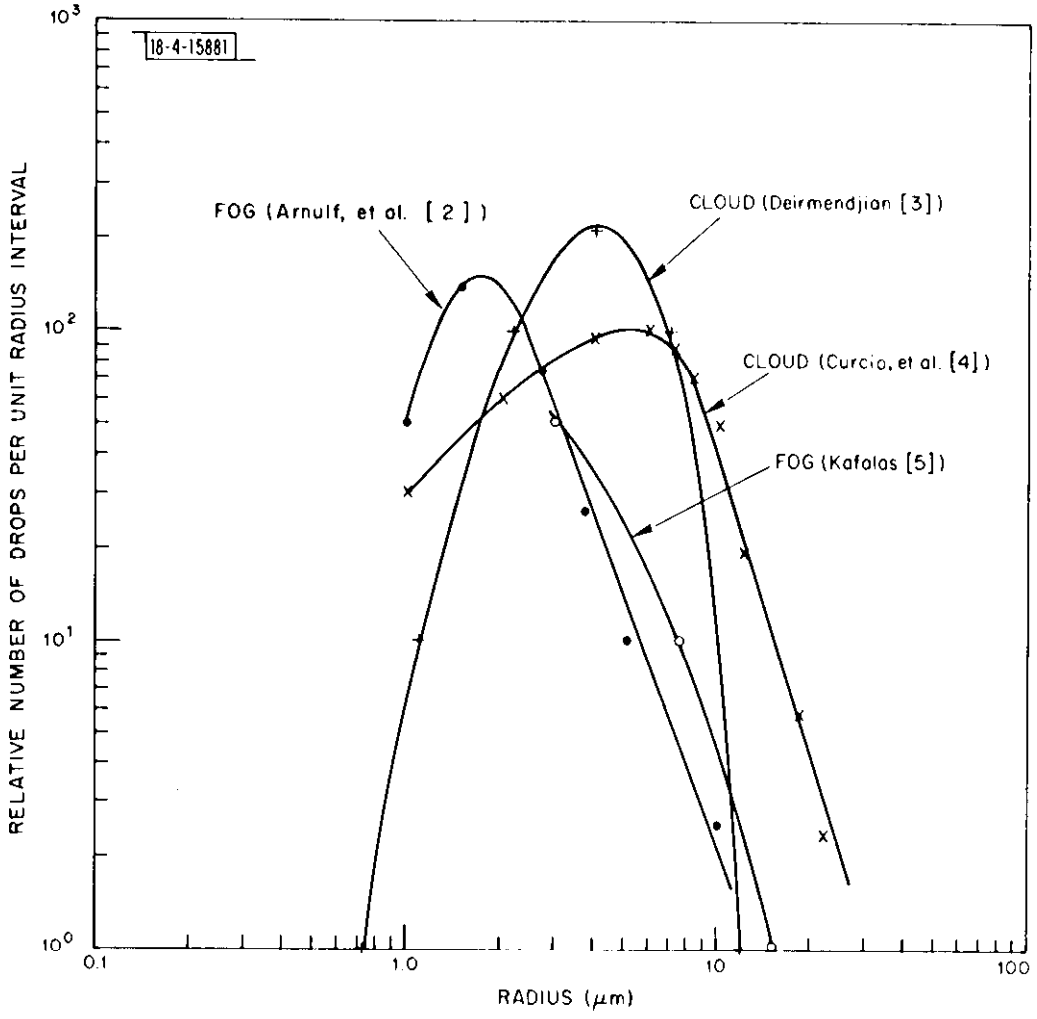

Fig. 3. Cloud and fog droplet size distributions from several sources.

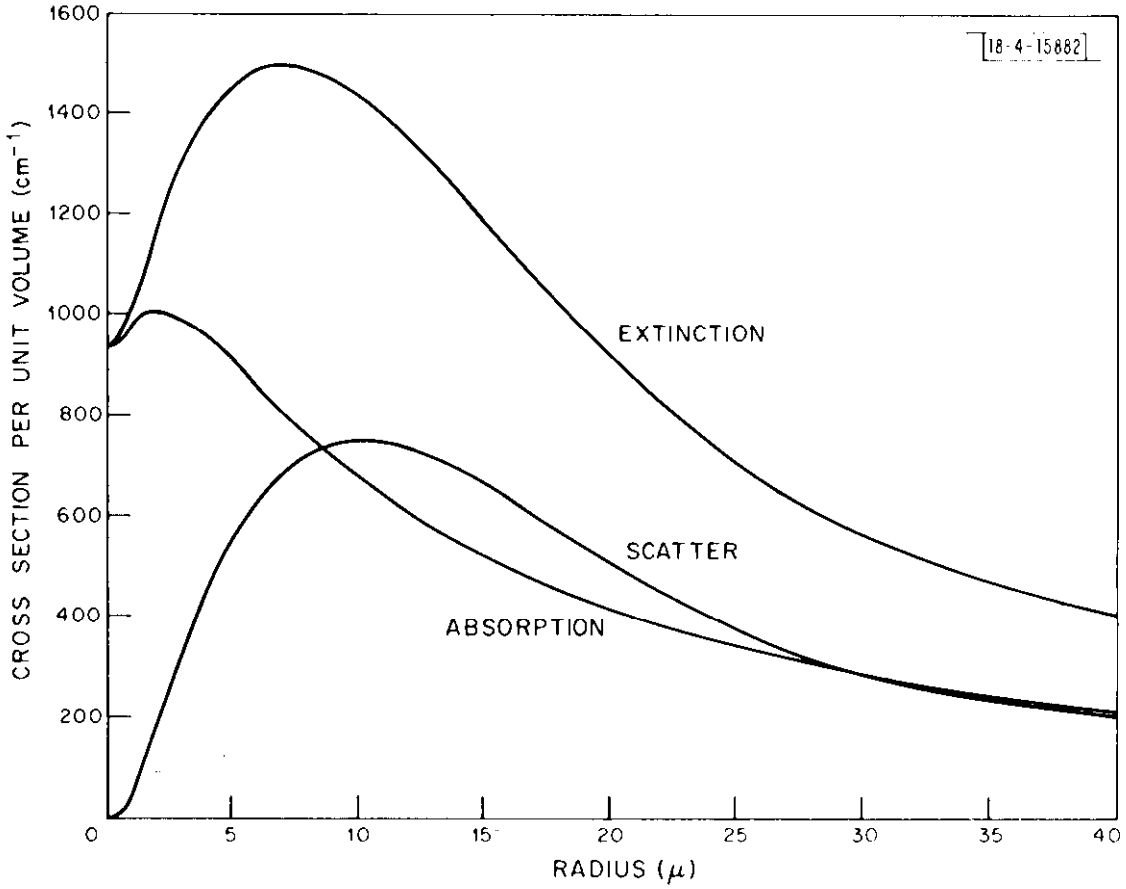

Fig. 4. Computed cross-section of water droplets at 10.6 μm.

that absorption by atmospheric water vapor is a source of significant attenuation.

To determine the attenuation at 10.6 μm the attenuation coefficient could be calculated as a function of visibility, but it is preferable to use experimental data. Arnulf et al.[2] measured light attenuation in a number of fogs as a function of wavelength. Their data for the attenuation at 0.5 μm have been replotted in Fig. 5. (Attenuation coefficient/km = [2.3] O.D./km.) For their data, it is seen that the attenuation coefficient in fogs at 10 μm ranges between 0.25 and 1.0 times the visible attenuation γ_v and lies between 0.5 and 1.0 times γ_v for 700 ft. daytime RVR fogs. Sanders and Selby[7] made simultaneous 0.63 μm and 10.6 μm laser transmission measurements through low clouds enveloping an experimental path located at 2,780 feet elevation. Their results are reproduced in Fig. 6 (Attenuation coefficient/km = [0.23] dB/km.) From their data, it appears the attenuation by clouds at 10.6 μm typically is 0.25 times the attenuation at 0.63 μm for the range of visibilities down to 700 ft. daytime RVR (visible attenuation <128 dB/km) and that nearly all the data in this visibility range lie below the line $\gamma_{10.6}/\gamma_{0.63} = 0.5$. The attenuation by water vapor at 10.6 μm is negligible compared to the attenuation by scattering for the fogs and clouds which reduce the visibility to Cat III-a minimums.

For wavelengths beyond 10.6 μm the ratio of droplet diameter to wavelength decreases and scattering by fog and cloud droplets diminishes rapidly. However, at these longer wavelengths water vapor absorption increases significantly. Apparently, at this time little information is available about laser transmission through water vapor in the 100-300 μm wavelength region because until very recently few lasers in this spectral region were available. Measurements have been reported by Burroughs et al.[13] for the CN laser (337 μm) which indicates the water vapor absorption at 0° C and 100% humidity is 50 dB/km. The same reference states the attenuation by scattering was 14 ± 5 dB/km for a fog in which the visual range for 2% contrast was 70 meters. Sanders and Selby[7] estimated the 337 μm attenuation by scattering was 20 ± 10 dB/km in thick cloud when the attenuation at 0.63 μm was 400 dB/km. These fogs and clouds are much more dense than Cat. III-a minimum clouds and fogs. These data indicate that as expected, attenuation by scattering in the far infrared is not an important consideration for the fogs and clouds being considered here. Furthermore, the water vapor absorption at

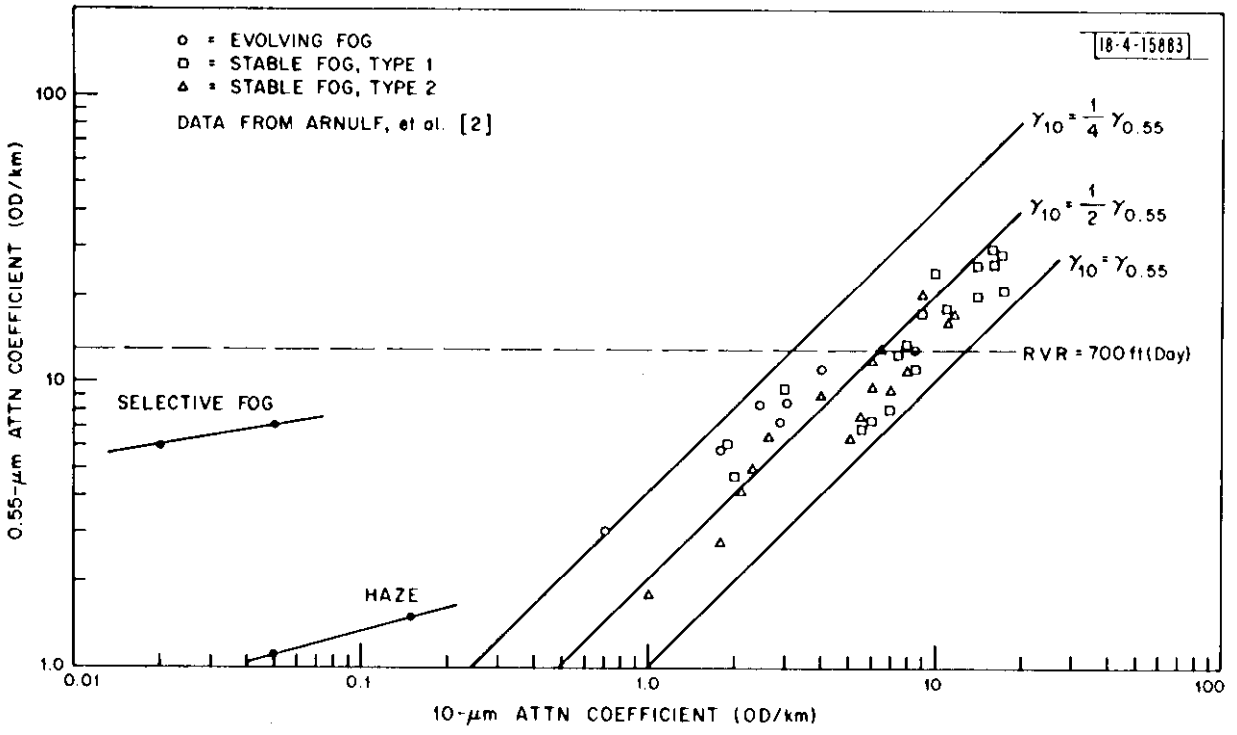

Fig. 5. Attenuation coefficient at 0.55 μm vs. attenuation coefficient at 10 μm for various fogs. (from [2]).

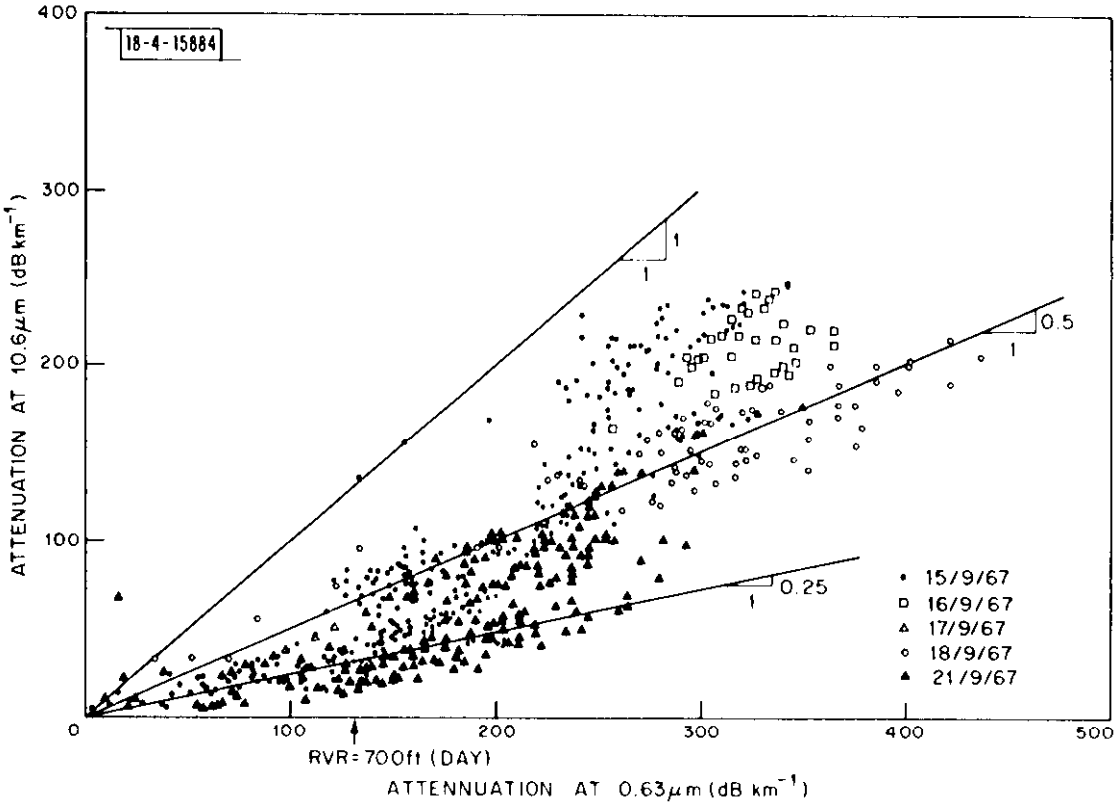

Fig. 6. Attenuation at 0.6 μm vs. attenuation at 10.6 μm for various cloud densities (from [7]).

337 μm (50 dB/km at 0°C) is comparable to typical 10.6 μm scattering and absorption losses, which range from 32 to 128 db/km in clouds and fogs having the minimum Cat III-a daytime RVR. For example, at 25°C the precipitable water vapor capacity of the air is more than four times greater than the capacity at 0°C, which predicts that at 25°C the water vapor absorption loss at 337 μm could be as great as 200 dB/km.

In conclusion, these data show that for fog and cloud densities corresponding to Cat III-a minimums values of A=0.5 are typical and that $\gamma_{10.6}/\gamma_{vis}$ may range from 0.1 to 1.0 depending on the droplet size distribution, typical values being 0.7 in fog and 0.25 in cloud. At long infrared wavelengths (337 μm) the attenuation by scattering from fogs and clouds diminishes considerably, but atmospheric water vapor can introduce an even larger attenuation. These facts suggest that 10.6 μm is a logical wavelength for the optical LGS model, especially since large laser powers are available. Calculations in the next section are based on this wavelength choice. If in the future, lasers of appreciable power, operating in "clear" atmospheric windows, become available in the region beyond 10.6 μm, this choice may have to be reexamined.

V. PERFORMANCE OF THE BASELINE OPTICAL LGS

To compute the optical LGS performance in a Cat. III-a fog, it is necessary to determine:

1. The attenuation of the signal by the fog
2. The amount of fog-scattered light entering the receiver
3. The amount of noise generated by the entry of background radiation into the receiver.

In this section these quantities are determined as a function of range, R, for a representative optical LGS operating at 10 μm wavelength.

The optical LGS is assumed to transmit from the ground a fan-shaped scanning beam having angular dimensions θ_t^{α} and θ_t^{β} in the azimuth and elevation directions, respectively. If the transmitted power is P_t, the power density at the receiver aperture in an airplane at range R is

$$\frac{P_t\, e^{-\gamma R}}{R^2\, \theta_t^{\alpha}\, \theta_t^{\beta}} \qquad (4)$$

where γ is the attenuation coefficient of the propagation medium. The scanning beam power P_s received by the receiver is

$$P_s = \frac{P_t A_r e^{-\gamma R}}{R^2 \theta_t^{\alpha} \theta_t^{\beta}} \qquad (5)$$

where A_r is the receiver collecting aperture area.

To compute the amount of scattered light entering the receiver, use is made of an approximation obtained by Heggestad[6] for computing the distribution of intensity for light passing through a cloud layer. In Heggestad's analysis, it is assumed the scattering is principally in the forward direction, which is the case for fogs and clouds at both 0.5 and 10.6 μm. By assuming in the LGS case that the fog or cloud is uniformly distributed between the transmitter and receiver, Heggestad's results reduce to [See Appendix B] :

$$p_{sc}(\alpha_r, \beta_r; \alpha_t, \beta_t) = \frac{3\, p_t(\alpha_t, \beta_t)\, e^{-\gamma R}(1-A)}{\pi^2 A^2 (\gamma R)^2 W^4 R^2} \cdot$$

$$\exp\left\{-2\left[\frac{(\alpha_r - \alpha_t)^2}{\sigma_\alpha^2} + \sqrt{3}\,\frac{(\alpha_r - \alpha_t)(\alpha_t R)}{\sigma_\alpha \sigma_x} + \frac{(\alpha_t R)^2}{\sigma_x^2}\right]\right\} \cdot \qquad (6)$$

$$\exp\left\{-2\left[\frac{(\beta_r - \beta_t)^2}{\sigma_\beta^2} + \sqrt{3}\,\frac{(\beta_r - \beta_t)(\beta_t R)}{\sigma_\beta \sigma_x} + \frac{(\beta_t R)^2}{\sigma_x^2}\right]\right\}$$

where $P_{sc}(\alpha_r, \beta_r; \alpha_t, \beta_t)$ = elemental power/steradian $-m^2$ received from direction direction α_r, β_r due to $p_t(\alpha_t, \beta_t)$

$p_t(\alpha_t, \beta_t)$ = power/steradian $-m^2$ transmitted in the direction α_t, β_t

α_t, β_t are orthogonal angular coordinates measured with respect to the LOS between the transmitter and the receiver

α_r, β_r are angles of arrival at the receiver, measured with respect to the LOS

γ = attenuation coefficient/unit distance

R = range between transmitter and receiver

A = albedo of the fog or cloud (See Appendix B)

W = second moment of the single particle forward scattering pattern (See Appendix B)

$$\sigma_\alpha^2 = \sigma_\beta^2 = A\gamma R W^2$$

$$\sigma_x^2 = \left(\sigma_\alpha^2 R^2\right)/3$$

The scattered power P_{sc} received in a receiver having aperture area A_r and FOV of angular size $\theta_r^\alpha \cdot \theta_r^\beta$ is obtained by integrating α_r, β_r α_t, β_t over θ_r^α, θ_r^β, θ_t^α, θ_t^β, respectively, in (6):

$$P_{sc} = \iiint\!\!\iint p_{sc}\, d\alpha_t\, d\beta_t\, d\alpha_r\, d\beta_r = \frac{3\, P_t\, A_r\, e^{-\gamma R(1-A)}\, (\theta_r^{\alpha} \cdot \theta_r^{\beta})}{\pi^2\, A^2\, (\gamma R)^2\, W^4\, R^2}$$

$$\cdot \frac{1}{\theta_t^{\alpha}\, \theta_r^{\alpha}} \iint_{\theta_r^{\alpha}\, \theta_t^{\alpha}} \exp\left\{ -2\left[\frac{(\alpha_r - \alpha_t)^2}{\sigma_\alpha^{\,2}} + \sqrt{3}\, \frac{(\alpha_r - \alpha_t)(\alpha_t R)}{\sigma_\alpha\, \sigma_x} + \frac{(\alpha_t R)^2}{\sigma_x^{\,2}} \right] \right\} d\alpha_t\, d\alpha_r$$

$$\cdot \frac{1}{\theta_t^{\beta}\, \theta_r^{\beta}} \iint_{\theta_r^{\beta}\, \theta_t^{\beta}} \exp\left\{ -2\left[\frac{(\beta_r - \beta_t)^2}{\sigma_\beta^{\,2}} + \sqrt{3}\, \frac{(\beta_r - \beta_t)(\beta_t R)}{\sigma_\beta\, \sigma_x} + \frac{(\beta_t R)^2}{\sigma_x^{\,2}} \right] \right\} d\beta_t\, d\beta_r \qquad (7)$$

In (7) it has been assumed the transmitted power P_t is uniformly distributed throughout the fan beam. The first term in (7) is the scattered power received in a small FOV if the transmitted beam were a narrow pencil beam. The last two terms in (7) are normalized factors which describe the changes in scattered light entering the receiver which occur when the transmitted beam or the receiver FOV is broadened. For this problem, these factors were integrated numerically on a computer.

The amount of receiver noise arising from background radiation will lie somewhere between a lower limit which is the photon noise of the background radiation and an upper limit which is of the order of the background itself if the background is non-uniform. The lower limit[12] is given by the photon noise equivalent power (NEP) for P_b watts of background power at the wavelength λ:

$$NEP = \sqrt{2(\Delta f)\, P_b \; \frac{hc}{n\lambda} \left(\frac{\exp\left(\frac{hc}{\lambda kt}\right)}{\exp\left(\frac{hc}{\lambda kt}\right) - 1} \right)} \qquad (8)$$

where Δf = detector bandwidth
h = Planck's constant
c = speed of light
n = quantum efficiency of the detector
k = Boltzmann's constant
T = background temperature, ^{o}K
λ = wavelength

The term in (8) containing the exponentials is close to unity at $\lambda = 10\ \mu m$, but increases to about 6.8 at $\lambda = 337\ \mu m$. The background power P_b received in a receiver having aperture area A_r and field of view $\theta_r^{\alpha} \cdot \theta_r^{\beta}$ is:

$$P_b = A_r \theta_r^{\alpha} \theta_r^{\beta} \int_{\Delta\lambda} N_\lambda \, d\lambda \qquad (9)$$

where N_λ is the spectral radiance of the background. Typical maximum values of N_λ are given below[12].

λ	N_λ	Background
0.7 μm	10^{-2} $\frac{\text{watts}}{\text{cm}^2\text{-ster-}\mu\text{m}}$	sunlit cloud (or fog)
10 μm	10^{-3} $\frac{\text{watts}}{\text{cm}^2\text{-ster-}\mu\text{m}}$	300°K sky or terrain
300 μm	10^{-6} $\frac{\text{watts}}{\text{cm}^2\text{-ster-}\mu\text{m}}$	300°K sky or terrain

Substituting (9) in (8), we see

$$\text{NEP} = \sqrt{(\Delta f) \int_{\Delta\lambda} N_\lambda \, d\lambda \, A_r \theta_r^{\alpha} \theta_r^{\beta} \, \frac{hc}{n\lambda} \left(\frac{\exp\left(\frac{hc}{\lambda kt}\right)}{\exp\left(\frac{hc}{\lambda kt}\right) - 1} \right)} \qquad (10)$$

The receiver mounted in the airplane is assumed to have an aperture two inches in diameter and, for the sake of simplicity, a FOV 20° by 20°. A spectral bandwidth $\Delta\lambda$ of 1 μm at 10 μm is assumed. The signal bandwidth Δf required for the elevation scanning beam was found in Section II to be about 2×10^4 Hz for a fan beamwidth of $1/2 \times 10^{-3}$ radian. Smaller beamwidths are not practical at 10.6 μm because of diffraction. (One half milliradian is only about two and a half times the diffraction limit of a two-inch aperture at 10.6 μm.) The quantum efficiency of the detector, n, is assumed to be 0.2.

The computed signal and noise powers for the elevation scanning fan beam optical LGS are plotted in Fig. 7 as a function of range and 10.6 μm attenuation using values of A and W from Appendix B. The transmitted laser power was assumed to be 100 watts. In Fig. 7 P_s is the attenuated direct signal power and P_{sc} is the scattered laser signal power at the receiver detector. The background noise power for this system is about 3×10^{-9} watts. In Section III, it was noted that when the daytime RVR is 700 feet, typical values of the 10 μm attenuation coefficient were $0.7\gamma_{vis}$ for fogs and $0.25\gamma_{vis}$ for clouds. This corresponds to 38/n. m. and 13.6/n. m., respectively. For night operations the attenuation coefficient would be twice as large for 700 foot RVR. The curves in Fig. 7 include a case for which $\gamma_{10.6\mu m} = 20$/n. m., which corresponds to a daytime RVR in fog of 1200 feet. For this case, it is seen that the direct signal has decreased to the background noise power at a range of 0.6 n. m., which is far short of the 2 n. m. goal.

Referring to Fig. 7, it is apparent that the signal is always significantly greater than the received scattered light power for the usable ranges when the signal is greater than the background equivalent noise power. If one attempts to increase the range by increasing the transmitted power, then both the signal and the scattered light will increase and the range is limited to approximately 0.85 n. m., the range at which they become equal.

Two variables under the control of the designer are the solid angles $(\theta_t)^2$ and $(\theta_r)^2$, the transmitter and receiver solid angle fields of view. A system in which the transmitted scanning fan beam is replaced by a "raster" scanning pencil beam (to reduce the value of θ_t^2) is one of the variations of the baseline system examined in the next section.

VI. ALTERNATIVES TO THE BASELINE SYSTEM

Inasmuch as the baseline optical LGS system performance was shown in Section V. to be inadequate in Cat. III-a minimums, a number of alternatives are examined here. Although none of these alternatives proved successful either, a discussion of them is included here for completeness.

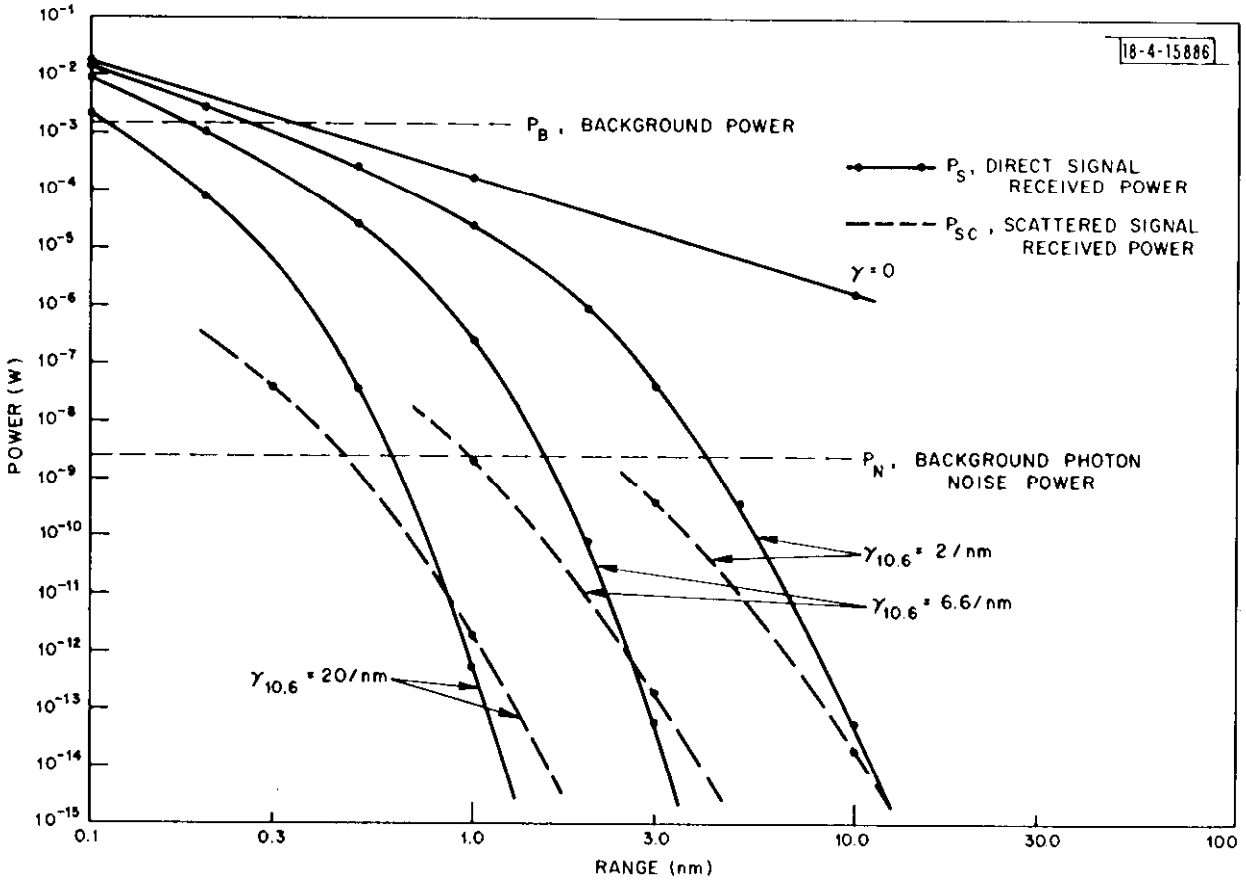

Fig. 7. Received signal power for scanning fan beam optical LGS.

——●——●——●—— P_S, direct signal received power.

- P_{SC}, scattered signal received power.

One way of increasing the signal power without increasing appreciably the scattered light is to reshape the fan beam into a pencil beam which performs a raster scan. Such a system probably requires a position message encoded on the beam, which in turn requires a wider receiver bandwidth. A pencil beam scanning system has been analyzed in which the beam diameter is the same as the thickness of the fan beam described earlier. The results are summarized in Fig. 8. The intensity of the signal is increased by a factor of 1.3×10^3, while the scattered light changed very little at the longer ranges. The pencil beam has approximately 4×10^6 address locations in the raster field, requiring an address bit rate of approximately 1.6×10^9 per second. The increase in receiver bandwidth necessary to accommodate this large bit rate results in an increase in the NEP, which consequently limits the range to 0.6 n. m., the same range obtained with the fan beam system. However, with the pencil-beam system a significant increase in transmitted power would permit operation out to about 1.4 n. m., at which range the scattered signal power becomes equal to the signal power. The required increase in transmitted power is a factor of approximately 10^7. All things considered, this alternative to the basic system does not appear feasible.

Another alternative is to decrease the receiver FOV, thereby reducing the scattered signal power. This is possible if a tracking receiver is used in the airplane. For practical purposes, the received scattered signal power in this case is proportional to the receiver FOV. For instance, if the receiver FOV were changed from $20^\circ \times 20^\circ$ to $2^\circ \times 2^\circ$, the scattered signal power would decrease by a factor of 10^2, and the background NEP would decrease by a factor of 10. Referring to Fig. 7 for the fan-beam scanning system, we see that even under these conditions the system range is still less than about 0.7 miles and that with unlimited transmitter power, the scattered light power would become equal to the signal power at slightly less than two nautical miles range.

If one postulates a coherent receiver system, then it is possible to reduce significantly the receiver NEP. However, the scattered signal power remains within the passband of the receiver and so remains unchanged. It appears doubtful even with a narrow FOV receiver that a range of two miles could be obtained when the RVR is 700 feet. In addition, the coherent receiving equipment is significantly more complex and expensive.

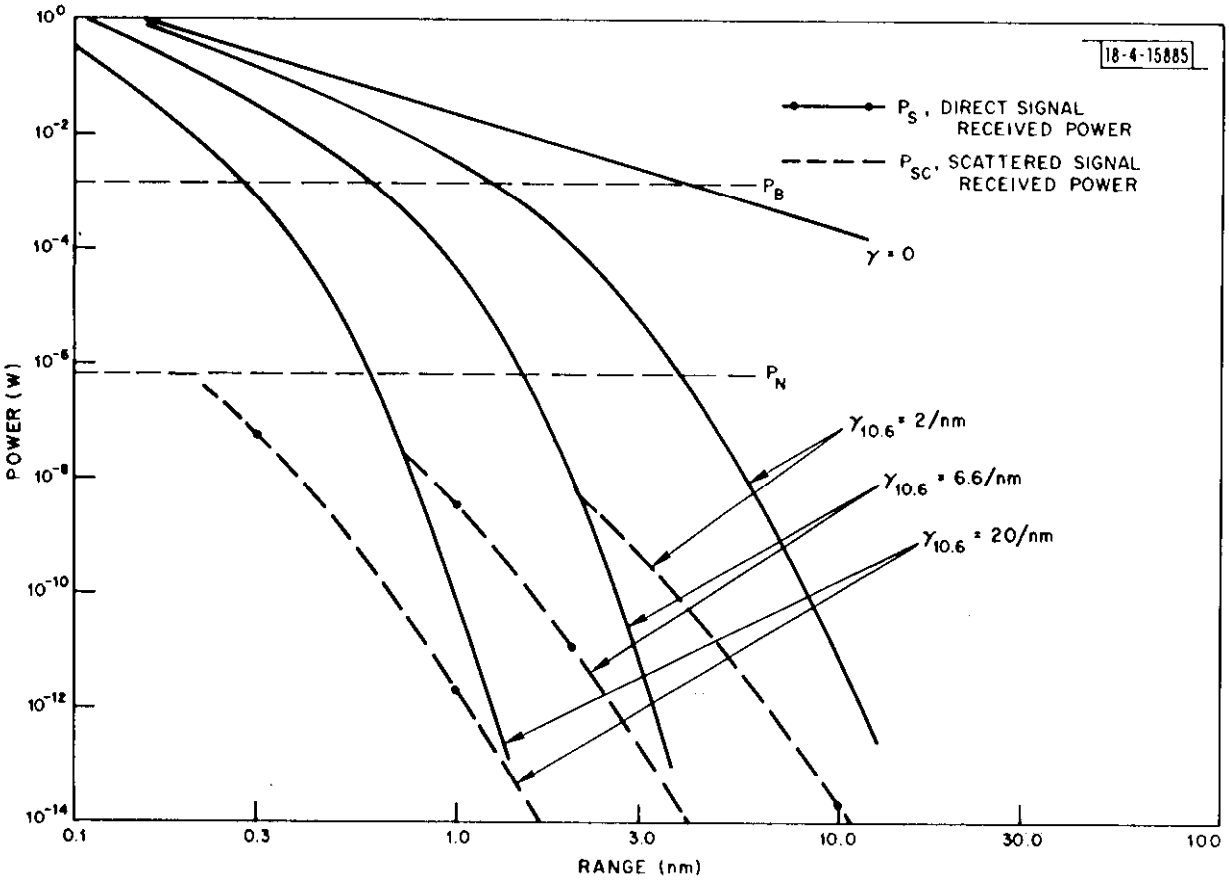

Fig. 8. Received signal power for scanning pencil beam optical LGS.

———●———●———●——— P_S, direct signal received signal.

- P_{SC}, scattered signal received power.

VII. CONCLUSIONS

It is concluded from this review of optical propagation through fog that an optical LGS providing reliable guidance at a range of two miles in Cat. III-a minimums is not possible with the technology considered here. At 10.6 μm, the fundamental limitation is the rapid attenuation of the signal by the fog. However, the scattered light power also becomes a significant factor before a range of two miles is reached. In reaching this conclusion, it was assumed the fog had characteristics which were the average of reported measurements. It is recognized that the characteristics of individual fogs differ significantly, but for purposes of computation here the values of γ and A used were the averages of typical values obtained experimentally.

While scattering by fog droplets decreases significantly at longer wavelengths, data at one far IR wavelength (337 μm) indicate that atmospheric water vapor absorption would be larger than the attenuation at 10.6 μm by a Cat. III-a fog. The far IR region is an area of active laser research, and water vapor attenuation at other discrete wavelengths should be forthcoming shortly. However, until a far IR window is found (if one exists), 10.6 μm remains the better choice, especially in view of the large amount of laser power available.

At wavelengths closer to the visible, the amount of scattered light, relative to the situation at 10.6 μm, is much larger. This increase occurs because both the albedo A and the attenuation coefficient γ are larger at visible wavelengths.

The conclusions reached here are based on the assumption of a spatially uniform fog or cloud. Because clouds and fogs can be extremely inhomogeneous, the additional problem of erroneous signals received via reflections must be a consideration in the further assessment of optical LGS techniques.

APPENDIX A

Various definitions of visibility are used for different applications. There are appreciable differences between some of these definitions, so use of the appropriate definition is important in the determination of the corresponding attenuation coefficient. References [8] and [9] discuss these definitions.

Atmospheric transmission is equal to exp (-γR), where γ is the attenuation coefficient. The same factor describes the reduction in contrast for a distant object. Thus, in the daytime for visual ranges greater than 3,827 feet, the visibility is defined, for RVR determination, as the range at which the contrast of a 100% white/black target is reduced to 0.05:

$$0.05 = e^{-\gamma(RVR)}$$

or

$$\gamma(RVR) = \ln(0.05) \qquad \text{A1}$$

At night and during poor visibility in daytime the RVR is determined from Allard's Law

$$E_t = \frac{Ie^{-\alpha(RVR)}}{\left(\frac{RVR}{5280}\right)^2} \qquad \text{A2}$$

where I is the intensity of the approach lighting in candelas and E_t is the illuminance threshold of the eye in mile-candles. For the approach lighting installed at Logan Airport (Step 5 lighting), and using the daytime and nighttime values of E_t, A2 becomes

$$\gamma = \frac{25.86}{(RVR)} - \frac{2 \ln (RVR)}{(RVR)} \quad \text{(nighttime)} \qquad \text{A3}$$

$$\gamma = \frac{19.4}{(RVR)} - \frac{2 \ln (RVR)}{(RVR)} \quad \text{(daytime)} \qquad \text{A4}$$

At RVR = 700 ft., Equations A3 and A4 give

$$\gamma = 1.8 \times 10^{-2}/\text{ft} = 109/\text{nm}, \text{ or } \frac{256 \text{ dB}}{\text{km}} \qquad \text{A5}$$

$$\gamma = 9 \times 10^{-3}/\text{ft} = 54.5/\text{ nm}, \text{or } \frac{128 \text{ dB}}{\text{km}} \qquad \text{A6}$$

for the attenuation in the visible portion of the optical spectrum.

APPENDIX B

Heggestad[6] has determined the approximate angular and spatial distribution of the scattered light arriving at a receiver on the ground from a cloud which is illuminated from above (such as from a satellite). The cloud was of uniform thickness T and its lower surface was at a height H above the ground (See Fig. B1 [a]). Heggestad assumed a Gaussian power distribution for the illumination from the direction (α_i, β_i) at the point (x_i, y_i) on the cloud top (See Eq. 49 in [6]). He then obtained an approximate distribution for the scattered light power incident on the ground beneath the cloud. Heggestad's results can be used in the optical LGS model by turning the cloud on its edge and assuming that the LGS transmitter is located on the "top" surface and that the receiver is at the "bottom" surface by setting H = 0 (See Fig. B1[b]).

By considering the transmitter aperture as the source of the incident illumination and noting that it corresponds to a Gaussian power distribution of negligible size (so $\sigma_{xi} \ll \sigma_{xG}$ in Heggestad's notation) Heggestad's result gives the following function for the incident power distribution at the receiver, $P_{sc}(\alpha_r, \beta_r, x_r, y_r; \alpha_t, \beta_t, x_t, y_t)$ (watts/steradian-m^2), due to one watt/steradian -m^2 radiated in the direction (α_t, β_t) from the point (x_t, y_t) in the transmitter aperture.

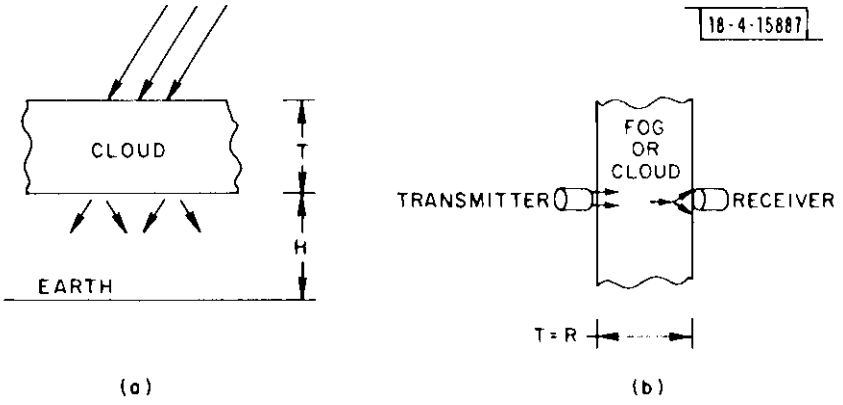

Fig. B1 Heggestad's cloud geometry adapted for the LGS problem.

$$P_{sc}(\alpha_r, \beta_r, x_r, y_r; \alpha_t, \beta_t, x_t, y_t) =$$

$$\frac{e^{-N_e(1-\gamma_f)}}{4\pi^2 \sigma_\alpha \sigma_\beta \sigma_{xG} \sigma_{yG} \sqrt{(1-\rho^2_{\alpha xG})(1-\rho^2_{\beta yG})}}$$

$$\exp\left\{-\frac{1}{2(1-\rho^2_{\alpha xG})}\left[\frac{(\alpha_r-\alpha_t)^2}{\sigma_\alpha^2} - 2\rho_{\alpha xG}\frac{(\alpha_r-\alpha_t)(x_r-x_t+R\alpha_t)}{\sigma_\alpha \sigma_{xG}} + \frac{(x_r-x_t+R\alpha_t)^2}{\sigma_{xG}^2}\right]\right\} \quad \text{(B1)}$$

$$\exp\left\{-\frac{1}{2(1-\rho^2_{\beta yG})}\left[\frac{(\beta_r-\beta_t)^2}{\sigma_\beta^2} - 2\rho_{\beta yG}\frac{(\beta_r-\beta_t)(y_r-y_t+R\beta_t)}{\sigma_\beta \sigma_{yG}} + \frac{(y_r-y_t+R\beta_t)^2}{\sigma_{yG}^2}\right]\right\}$$

where for H = 0 and T = R,

x, y are measured from the center of the transmitter or receiver apertures

α, β are orthogonal angular coordinates measured with respect to the LOS. (See Reference [6]).

N_e = cloud optical thickness = γR

γ_f = average forward scattering efficiency (see below)

$\sigma_\alpha^2 = \sigma_\beta^2 = \gamma_f N_e W^2$

$\sigma_{xG}^2 = \sigma_x^2 = \gamma_f N_e W^2 R^2/3$

$\rho_{\alpha xG} = \rho_{\beta yG} = -\frac{1}{2}\cdot\sqrt{3}$

W = scattering pattern width factor (see below)

A number of approximations were used both by Heggestad and this author to obtain this result, including the approximation $\alpha \approx \sin\alpha$ and $\beta \approx \sin\beta$, which restricts the solution to $\pm$ 1 radian. Heggestad's original report[10] should be consulted for the application of this result to other problems.

In Eq. B1, γ_f is the ratio of the average forward scattering cross section to the average extinction cross section for the scattering particles. For fog and cloud droplets at both visible wavelengths (See Heggestad[10]) and 10 μm (See Diermendjian[3]) essentially all the scattered energy is directed into the forward hemisphere. Thus in these cases the albedo A (average scattering cross section/average extinction cross section) is very nearly equal γ_f and A is used in place of γ_f in the scattered power computation. W, the forward scattering pattern "width" parameter, is the second moment of the normalized forward scattering pattern. Heggestad[10] obtained W = 0.295 radian for fog and cloud droplets at visible light wavelengths. Using Diermendjian's[3] cloud droplet scattering patterns, this author obtained the values W = 0.193 and 0.15 at 10.0 and 0.7 μm wavelength, respectively.

Equation B1 can be simplified somewhat by noting $[\,(x_r - x_t)/\sigma_{xG}\,] \ll 1$ for this problem. x_r and x_t represent position in the receiver and transmitter apertures, both of which are probably smaller than 0.1 meter. Using

$$\gamma_f = 0.6$$

$$\gamma = 50/\text{km (attenuation in fog at 10 } \mu\text{m during Cat. III-a minimums)}$$

$$R = 1.0 \text{ km}$$

$$W = 0.193$$

we find

$$\sigma_{xG} = \sqrt{\gamma_f \gamma R \cdot WR/\sqrt{3}}$$

$$\approx 300 \text{ meters}$$

Therefore, the term $(x_r - x_t)/\sigma_{xG}$ cannot cause those exponential factors in B1 to be appreciably smaller than unity and hence they may be deleted from the exponent. Making these substitutions, B1 becomes

$$P_{sc}(\alpha_r, \beta_r, x_r, y_r; \alpha_t, \beta_t, x_t, y_t)$$

$$= \frac{3 \exp\left\{-\gamma R (1-A)\right\}}{\pi^2 A^2 (\gamma R)^2 W^4 R^2}$$

$$\cdot \exp\left\{-2\left[\frac{(\alpha_r - \alpha_t)^2}{\sigma_\alpha^2} + \sqrt{3}\,\frac{(\alpha_r - \alpha_t)(R\alpha_t)}{\sigma_\alpha \sigma_x} + \frac{(R\alpha_t)^2}{\sigma_x^2}\right]\right\}$$

$$\cdot \exp\left\{-2\left[\frac{(\beta_r - \beta_t)^2}{\sigma_\beta^2} + \sqrt{3}\,\frac{(\beta_r - \beta_t)(R\beta_t)}{\sigma_\beta \sigma_y} + \frac{(R\beta_t)^2}{\sigma_y^2}\right]\right\} \qquad (B2)$$

In Section V, Eq. B2 is integrated over the angular distribution of the optical LGS transmitter fan-shaped beam and over the receiver FOV to obtain the total scattered light power entering the receiver.

REFERENCES

1. T. S. Chu and D. C. Hogg, "Effects of Precipitation on Propagation at 0.63, 3.5 and 10.6 Microns," Bell System Tech. J. 47, 723 (1968).

2. A. Arnulf, J. Bricard, E. Curé and C. Véret, "Transmission by Haze and Fog in the Spectral Region 0.35 to 10 Microns," J. Opt. Soc. Am. 47, 491 (1957).

3. D. Deirmendjian, "Scattering and Polarization Properties of Water Clouds and Hazes in the Visible and Infrared," Appl. Opt. 3, 187 (1964).

4. J. A. Curcio, G. L. Knestrick and T. H. Cosden, "Atmospheric Scattering in the Visible and Infrared," NRL Report 5567 (24 January 1961), DDC AD-250945.

5. Optics Research Report, Lincoln Laboratory, M. I. T. (1971:2), p. 21, DDC AD-901213.

6. H. M. Heggestad, "Multiple-Scattering Model for Light Transmission Through Optically Thick Clouds," J. Opt. Soc. Am. 61, 1293 (1971).

7. R. Sanders and J. E. A. Selby, "Comparative Measurements of the Attenuation of Visible and Infrared Laser Radiation in Cloud," Systems Research Division, E. M. I., Ltd. (1968).

8. G. T. Schappert "Visibility Concepts and Measurement Techniques for Aviation Purposes," Department of Transportation, Report No. DOT-TSC-FAA-71-25 (July 1971).

9. H. O. Curtis and R. S. Kennedy, "Predictions of Laser Gate Performance," Technical Report 73-1, Harrington, Davenport and Curtis, Inc., Bedford, Mass. (8 January 1973).

10. H. M. Heggestad, "Optical Communication Through Multiple Scattering Media," Technical Report 472, Research Laboratory of Electronics, M. I. T. (22 November 1968).

11. Optics Research Report, Lincoln Laboratory, M. I. T. (1970:3), p. 21, DDC AD 882617.

12. W. L. Wolfe, ed. "Handbook of Military Infrared Technology," Office of Naval Research, Washington, D. C. (April 1965).

13. W. J. Burroughs, E. C. Pyatt and H. A. Gebbie, "Transmission of Submillimeter Waves in Fog." Nature 212, 387-8 (1966).

DOCUMENT CONTROL DATA - R&D

(Security classification of title, body of abstract and indexing annotation must be entered when the overall report is classified)

1. ORIGINATING ACTIVITY *(Corporate author)* Lincoln Laboratory, M.I.T.	2a. REPORT SECURITY CLASSIFICATION Unclassified 2b. GROUP

3. REPORT TITLE

Prediction of Optical Landing Guidance System Performance in Cat. III-a Minimum Weather

4. DESCRIPTIVE NOTES *(Type of report and inclusive dates)*
Technical Note

5. AUTHOR(S) *(Last name, first name, initial)*

Kocher, David G.

6. REPORT DATE 8 November 1973	7a. TOTAL NO. OF PAGES 38	7b. NO. OF REFS 13
8a. CONTRACT OR GRANT NO. F19628-73-C-0002 b. PROJECT NO. 649L c. d.	9a. ORIGINATOR'S REPORT NUMBER(S) Technical Note 1973-47 9b. OTHER REPORT NO(S) *(Any other numbers that may be assigned this report)* ESD-TR-73-258	

10. AVAILABILITY/LIMITATION NOTICES

Approved for public release; distribution unlimited.

11. SUPPLEMENTARY NOTES None	12. SPONSORING MILITARY ACTIVITY Air Force Systems Command, USAF

13. ABSTRACT

The feasibility of using a laser optical system to provide precision guidance for the final two miles of aircraft landing approaches in low visibility weather is examined. Since low visibility is caused most frequently by clouds and fog, approximate calculations of the optical signal, scattered light and noise are made as a function of range for various cloud and fog densities. It is concluded that with current laser technology, performance of an optical landing guidance system would be inadequate in the presence of Category III-a minimum visibility clouds and fogs.

14. KEY WORDS

optical landing guidance system
air traffic control
laser technology
low visibility weather